Journal of Porphyrins and Phthalocyanines
J. Porphyrins Phthalocyanines 2012; **16**: 589–602
DOI: 10.1142/S1088424612500733

Published at http://www.worldscinet.com/jpp/

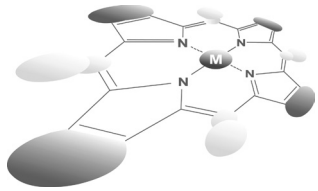

The long and winding road to new porphycenes

Igor Czerski[a], Arkadiusz Listkowski[a,b], Jan Nawrocki[a], Natalia Urbańska[a], Hubert Piwoński[a], Adam Sokołowski[a], Oksana Pietraszkiewicz[a], Marek Pietraszkiewicz*[a] and Jacek Waluk*[a,b◊]

[a] *Institute of Physical Chemistry, Polish Academy of Sciences, Kasprzaka 44/52, Warsaw 01-224, Poland*
[b] *Faculty of Mathematics and Natural Sciences, College of Science, Cardinal Stefan Wyszyński University, Dewajtis 5, Warsaw 01-815, Poland*

Dedicated to Professor Emanuel Vogel in memoriam

Received 9 October 2011
Accepted 10 February 2012

ABSTRACT: We describe attempts — not always successful — made over the years to improve the efficiency of porphycene synthesis and to produce novel compounds, custom-designed for specific purposes. New porphycenes are reported, some of them obtained rather unexpectedly as by-products of the planned reactions. Structure and energy computations of possible tautomeric forms in porphycenes substituted by one, two, three, and four *tert*-butyl groups lead to predictions regarding the kinetics and mechanisms of intramolecular double hydrogen transfer. The occurrence of tautomerization in single molecules of *tert*-butyl-substituted porphycenes is demonstrated by using fluorescence polarization techniques.

KEYWORDS: porphycene, synthesis, tautomerism, photodynamic therapy, porphyrin isomers, McMurry, single molecule spectroscopy.

INTRODUCTION

The synthesis of porphycene by Emanuel Vogel and coworkers [1] has created a new branch of chemical research, devoted to the studies of constitutional isomers of porphyrin [2–9]. In a theoretical paper [10], inspired by the work of Vogel, all other possible "nitrogen-in" isomers have been discussed (Scheme 1), all except porphyrin (**1**) and porphycene (**2**) nonexistent at that time. Since then, three more have been synthesized (as alkyl or aryl derivatives): hemiporphycene (**3**) [11, 12] corrphycene (**4**) [13, 14], and isoporphycene (**5**) [15, 16], but three (**7–9**) still await experimental realization. Another isomer has also been obtained, characterized by one nitrogen atom located outside the inner cavity; it was dubbed "inverted" [17] or "N-confused" [18] porphyrin (**6**).

Porphyrins have been suitably described as "pigments of life" [19]; it was therefore to be expected that their isomers can prove useful in those areas where the interaction of light and matter is crucial. Indeed, porphycene derivatives turned out to be extremely promising in photodynamic therapy (PDT) [20]. For example, derivatives carrying methoxyethyl side chains were found to be between 17 and 220 times more active against SSK2 murine fibrosarcoma cells than Photofrin, one of the few approved and clinically used sensitizers [21]. Interestingly, this result cannot be solely due to a better absorption of porphycenes in the red part of the spectrum, because the absorption coefficients differ only by a factor of about ten. Moreover, the yields of single oxygen generation are lower in porphycenes [22]. Evidently, structural differences may lead to different kinetics of cell membrane penetration, and to different localization inside the cell. Studies of structure-properties

◊SPP full member in good standing

*Correspondence to: Marek Pietraszkiewicz, email: pietrasz@ichf.edu.pl, fax: +48 22-343-3333 and Jacek Waluk, email: waluk@ichf.edu.pl, fax: +48 22-343-3333

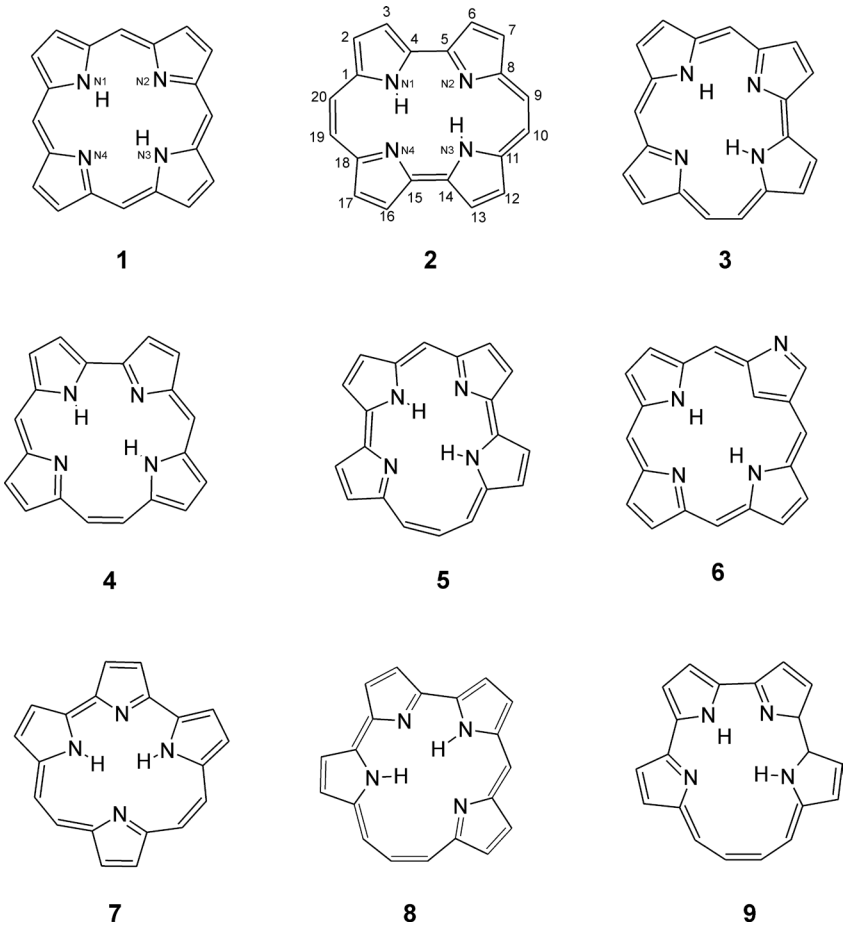

Scheme 1.

correlations require testing of differently substituted porphycenes.

Another area where the research on porphycenes has been very intense concerns tautomerism and hydrogen bond studies [9,23–60]. Two internal hydrogens can migrate between the four inner nitrogen atoms. Formally, this process is the same as in free-base porphyrins, but both the kinetics and the mechanism are totally different. In porphyrin, the ground state tautomerization proceeds in microseconds as a stepwise process [61–63], whereas in porphycenes two hydrogen move in a concerted fashion, and the reaction rates range between 10^{10} and 10^{13} s^{-1} [49, 56, 59]. This huge acceleration is caused by very strong intramolecular hydrogen bonds in porphycene. Variations of the rate constants over four orders of magnitude are suggestive of tunneling. In fact, studies of porphycenes isolated in supersonic jets [29, 37] and helium nanodroplets [53] revealed tunneling splittings. Most interesting was the finding that the splittings are vibrational-mode-specific: excitation of certain modes lowers the tautomerization barrier, for other modes the barrier is not influenced, and finally, it becomes higher for some vibrations. All these results make porphycenes role models for detailed studies of multidimensional double hydrogen tunneling. In addition, tautomerization in porphycenes can also be monitored on a single molecule level [36, 51]. On the application side, using tautomerization in porphycenes for construction of ultrafast switches has been proposed [58]. A related possibility, described in several patent applications, is to employ porphycenes for information storage.

The above examples show the importance of obtaining new porphycenes, custom-designed for specific purposes. Unfortunately, syntheses of porphycenes are rather difficult. They are usually based on the McMurry reductive cyclization of two 2,2′-bipyrrole moieties bearing carbonyl substituents in 5,5′-positions. The yields are small: 2–3% was reported for the parent porphycene [1]. The amount of the product can be enhanced by substituents in the pyrrole rings, the more bulky ones leading to higher yields. Thus, 10% has been reported for 2,7,12,17-tetrapropylporphycene [64], whereas the formation of 2,7,12,17-tetra-*tert*-butylporphycene (**10**) occurs with 20% yield [65]. Noting this higher yield, we produced parent porphycene by first obtaining 2,7,12,17-tetra-*tert*-butylporphycene and then removing the *tert*-butyl groups [66]. A similar approach has been employed earlier for the preparation of parent porphyrin [67, 68] and for the unsubstitued "inverted" isomer [69].

In this work, we describe the attempts to (i) optimize the yields in the syntheses of porphycenes and their building blocks; (ii) produce new compounds, relevant for the studies of tautomerization, hydrogen bond properties, spectroscopy, photophysics, and photodynamic therapy. Several new porphycenes are described; interestingly, some of them have been obtained somewhat by chance, as unexpected reaction by-products. We then focus on those molecules which exhibit lower symmetry, and thus different potential governing the intramolecular double hydrogen transfer. The results of calculations of optimized ground state geometry are presented for *trans* and *cis* tautomeric forms of *tert*-butyl-substituted porphycenes. On the basis of the analysis of relative energies and structural parameters, conclusions are presented regarding the tautomerization kinetics and mechanism: concerted *vs.* stepwise. Finally, using single molecule spectroscopy with polarized light, we show that tautomerization can be observed not only for porphycenes exhibiting symmetric double minimum potential, but also for asymmetrically substituted derivatives.

RESULTS AND DISCUSSION

Attempts to use Wittig reaction and its modifications

Based on the literature synthesis of 2,2′-(*Z*)-ethene-1,2-diylbis(1H-pyrrole) (**13**, Scheme 2), [70] we decided to use the Wittig reaction and its modifications for the synthesis of porphycenes.

We performed a series of control reactions on model compounds. In the study, we obtained derivatives of 2,2′-(*Z*)-ethene-1,2-diylbis(1H-pyrrole) **13**, but it turned out that pyrrole phosphorus ylide derivative (or phosphonate) must be protected on the nitrogen atom. The

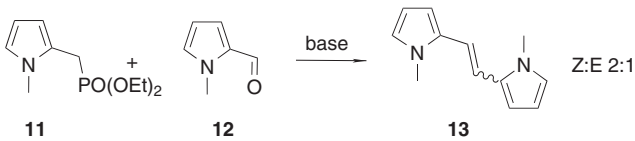

Scheme 2.

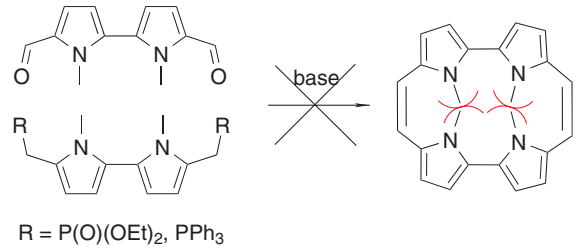

Scheme 3.

lack of protection makes the compounds so unstable that they decompose during the reaction, or during attempts at purification using traditional chromatographic methods. From the viewpoint of syntheses of porphycenes, nitrogen in the pyrrole ring cannot be associated with substituents larger than hydrogen: for steric reasons, this would make impossible the process of cyclization reaction shown in Scheme 3.

Attempts to use methathesis

In the next stage of research we decided to use a metathesis reaction leading to the transformation of porphycene, according to the synthetic pathways shown in Scheme 4.

In order to identify potential applications of this transformation we conducted a series of model reactions (Scheme 5). As catalysts, we used commercially available ruthenium complexes (Fig. 1). It should be noted that this is the first case of the use of metathesis reactions using unprotected vinyl pyrrole derivatives. The reactions were carried out in both homo-and cross-metathesis.

The highest yield (25%) was obtained for (*E*)-3-(1H-Pyrrol-2-yl)-acrylic acid ethyl ester (**14a**) [71] using an indenylidene catalyst, wherein the ratio of *E* to *Z* was 1/3. As a result of cross-metathesis reaction leading to compounds **17a** and **17b**, only *E*,*E* and *E*,*Z* products were obtained, not suitable for our purposes. Notwithstanding the low yield of metathesis, we attempted a synthesis of porphycene from "vinyl derivatives of bipyrrole" (Scheme 6). However, despite repeated attempts, no expected macrocycle was obtained. Getting porphycene requires two *Z* double bonds in the precursors. The

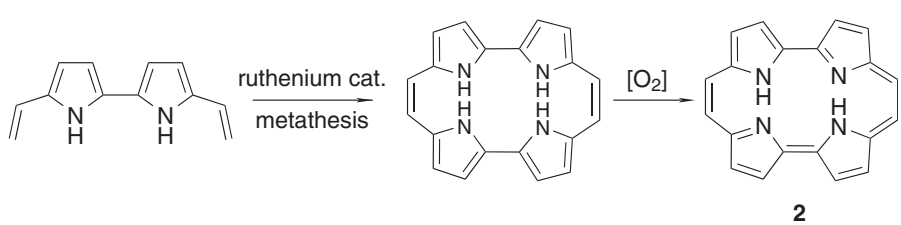

Scheme 4.

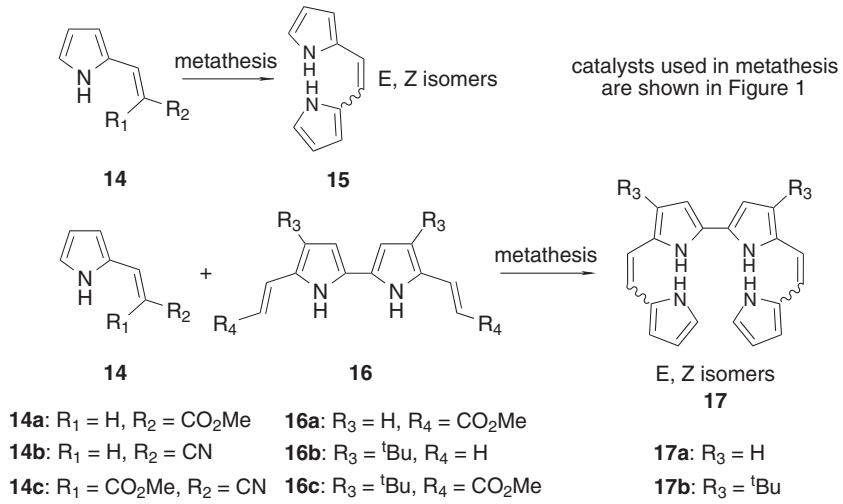

Scheme 5.

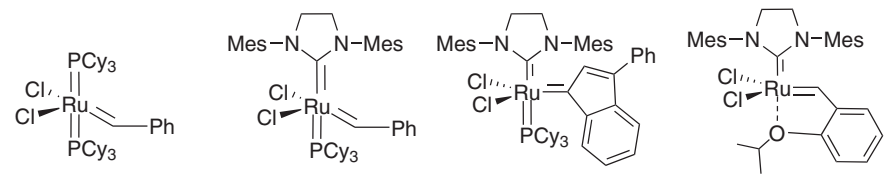

Fig. 1. The catalysts used in the thesis

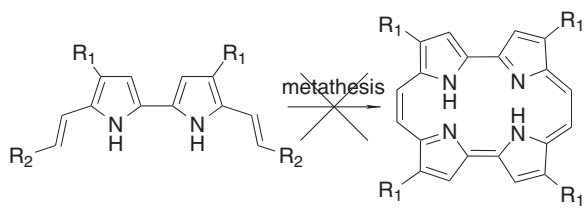

Scheme 6.

probability of obtaining such a system is very low due to the preferential formation of *E* double bond. Such precursors lead to the formation of polymers.

Synthesis of singly, doubly, and triply *tert*-butyl-substituted porphycenes

In the reaction of 2,7,12,17-tetra-*tert*-butylporphycene (**10**) with hot sulfuric acid we obtained remarkable amount of the unsubstituted porphycene [66] and a mixture of derivatives of not fully removed alkyl groups: 2-*tert*-butylporphycene (**18**), di-*tert*-butylporphycene — three regioisomers (**19**, **20**, **21**) and 2,7,12-tri-*tert*-butylporphycene (**22**) (Scheme 7). The amount of mono- di- and trisubstituted derivatives could be modified by changing the reaction conditions, e.g., reducing the temperature or shortening the reaction time.

It was feasible to isolate mono-substituted **18** and tri-*tert*-butylporphycene **22**. The mixture of disubstituted porphycenes has also been isolated, but the separation of individual regioisomers was not possible. However, we

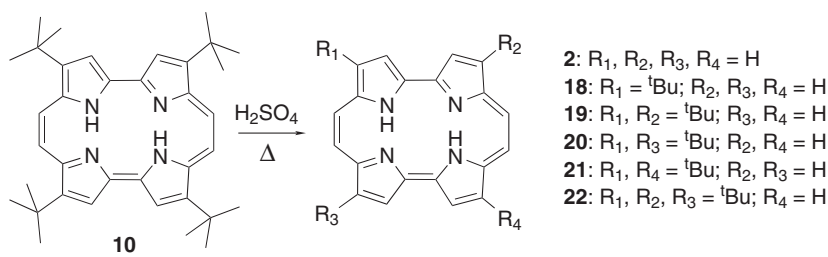

Scheme 7.

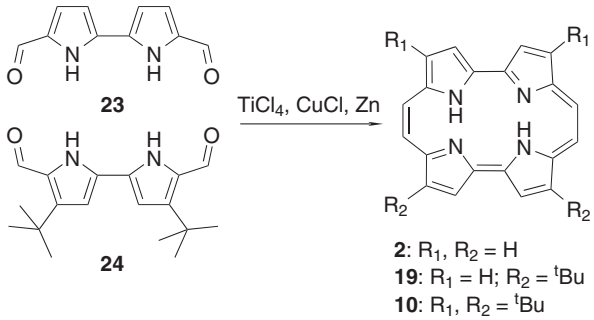

Scheme 8.

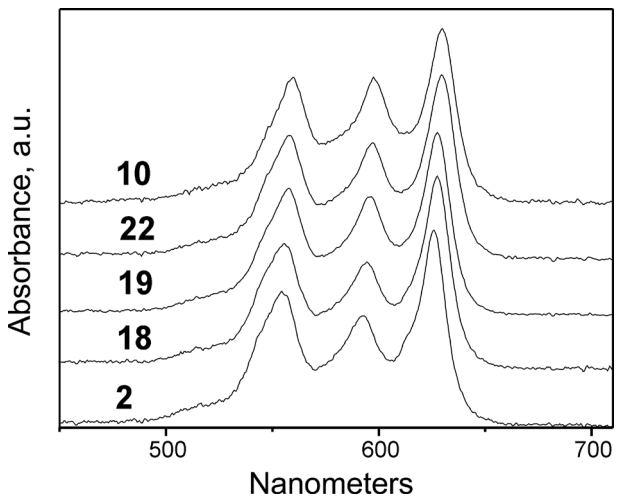

Fig. 2. The electronic absorption spectra in the Q region, recorded in acetonitrile at 293 K. From bottom to top: porphycene (**2**), 2-*tert*-butylporphycene (**18**), 2,7-di-*tert*-butylporphycene (**19**), 2,7,12-tri-*tert*-butylporphycene (**22**), 2,7,12,17-tetra-*tert*-butylporphycene (**10**)

synthesized 2,7-di-*tert*-butylporphycene **19** according to the reaction shown in Scheme 8.

Substituting porphycene by *tert*-butyl groups in β positions (2,7,12,17) has no significant impact on the shape and location of spectral bands (Fig. 2). In the electronic absorption spectra of unsubstituted porphycene (**2**), 2-*tert*-butylporphycene (**18**), 2,7-di-*tert*-butylporphycene (**19**), 2,7,12-tri-*tert*-butylporphycene (**22**) and 2,7,12,17-tetra-*tert*-butylporphycene (**10**) small shifts in the position of Q-bands towards lower frequencies are observed. The shapes of the bands remain almost identical.

With the increasing number of alkyl groups, evident shift of the Soret bands is observed toward longer wavelengths, exceeding 10 nm between porphycene (**2**) and 2,7,12,17-tetra-*tert*-butylporphycene (**10**) (Fig. 3).

Structure and tautomerism of *tert*-butyl-substituted porphycenes

In parent porphycene, symmetry dictates that two *trans* tautomers, with the inner protons located either at N1 and N3 or at N2 and N4 are chemically equivalent. Similarly,

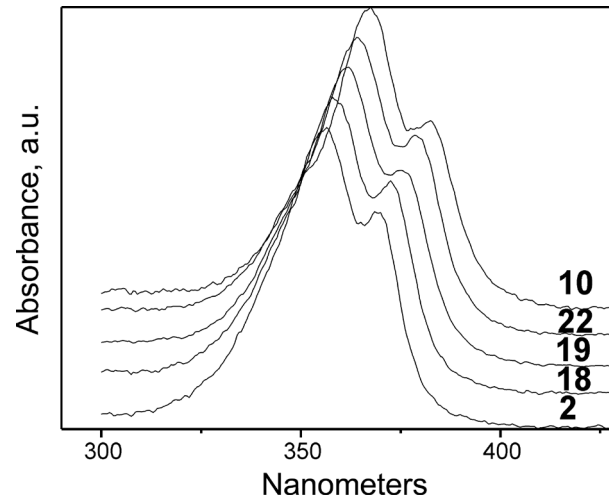

Fig. 3. The electronic absorption spectra in the Soret region, recorded in acetonitrile at 293 K. From bottom to top: porphycene (**2**), 2-*tert*-butylporphycene (**18**), 2,7-di-*tert*-butylporphycene (**19**), 2,7,12-tri-*tert*-butylporphycene (**22**), 2,7,12,17-tetra-*tert*-butylporphycene (**10**)

for the *cis* forms the same species correspond to the location of protons at N1 and N2 or N3 and N4 (for numbering, see Scheme 1). Another pair of equivalent *cis* tautomers is obtained by placing the protons either at N1 and N4 or N2 and N3. The latter structures lie at much higher energy than the other two pairs and are therefore not populated in the ground state, although they may play a crucial role in the radiationless deactivation of the excited state [52].

The pairwise degeneracy is broken for some *tert*-butyl-substituted porphycenes. In the monosubstituted derivative **18** both *trans* and *cis* tautomeric forms should have different energies. The same situation is encountered for **22**, the compound bearing three *tert*-butyl groups. In doubly substituted derivatives, lifting of degeneracy is expected for the *trans* forms of **21** and for the *cis* forms of **19**, whereas for **20** the pairwise symmetry should be preserved. In order to estimate the magnitude of these effects we optimized the geometry for the *trans* and *cis* structures of **2**, **10**, **18–22**. The results of calculations of relative energies (Table 1), inner cavity parameters (Table 2), and dipole moment values (Table 3), confirm the above considerations. For all the derivatives, the *cis-trans* energy difference is quite similar to that in the parent porphycene **2**; the largest differences, about 0.2 kcal/mol, are predicted for **21** and **10**. On the other hand, the energy splittings caused by lower symmetry are quite substantial, above 0.7 kcal/mol for the *trans* forms of **21** and about 0.4 kcal/mol for **18** and **22**. These numbers indicate that the asymmetry effects caused by a *tert*-butyl group are additive: in the doubly substituted porphycene **21** the stabilization of one *trans* tautomer *vs*. the other is about twice as large as in monosubstituted derivatives **18** and **22**. Interestingly, the computed splittings are much lower for the inequivalent *cis* forms.

While the energy difference of less than 1 kcal/mol may at first seem not very significant, we recall

Table 1. Calculated energy differences (in kcal/mol) between different tautomeric forms of parent and *tert*-butyl-substituted porphycenes. In *trans1*, the inner protons are located at N1 and N3, in *trans2*, at N2 and N4 (cf. Scheme 1). In *cis1* the protons reside on N1 and N2, in *cis2,* on N3 and N4

	ΔE(*cis1-trans1*)	ΔE(*trans2-trans1*)	ΔE (*cis2-cis1*)
2	2.24 (1.59)[a]	0	0
18	2.37 (1.77)	0.38 (0.41)	-0.02 (0.02)
19	2.15 (1.49)	0	-0.01 (0.07)
21	2.45 (1.89)	0.72 (0.79)	0
20	2.10 (1.47)	0	0
22	2.23 (1.60)	0.37 (0.35)	0.01 (0.07)
10	2.03 (1.37)	0	0

[a]In parentheses, the values obtained after zero-point-energy correction.

that the experimentally determined activation energy for tautomerization in parent porphycene is about 0.5 kcal/mol [42]. This finding led to postulating that double hydrogen transfer occurs *via* vibrational gating of concerted tunneling. Therefore, lifting of symmetric double minimum character for the potential of tautomerization may have dramatic consequences for both the kinetics and the mechanism of the reaction. This conjecture is strengthened by the analysis of the geometry of the inner cavity (Table 2). The values of NH–N distances and NHN angles, crucial for the rate of tautomerization, change upon substitution in a way which may either accelerate or slow down the process. For instance, the N1N4/N2N3 distances in the *trans* forms of **18** are longer than in parent **2**, whereas they become shorter for **22**. We have demonstrated [49] that very small variations of the inner cavity parameters lead to large changes in the tautomerization rates: upon passing from **2** to **10**, the rate of the ground state process increases from 5.8×10^{11} s^{-1} to 13.7×10^{11} s^{-1}, and the rate in S_1 from 7.4×10^{10} s^{-1} to 2.0×10^{11} s^{-1}. Comparison of the calculated geometry parameters of **2** with those of **10**, **18** and **22** leads to a prediction of the variability of tautomerization rates in singly and triply substituted porphycenes being greater than in the tetra-*tert*-butyl derivative. Moreover, the mechanism of the reaction need not be the same in all compounds. Inspection of Table 2 reveals for the *trans* form of **20** a large disparity between the N1N4 and N2N3 distances (267.0 and 264.1 pm, respectively). For such a case, the exchange of the two inner hydrogens may no longer be concerted, and the

Table 2. Calculated geometries of the inner cavity for different tautomeric forms of parent and *tert*-butyl-substituted porphycenes

	N1N4[a]	N2N3	N1N2	N3N4	NH1/NH2	N1HN4[b]	N2HN3
2-*trans*	265.5	265.5	283.8	283.8	104.9	152.6	152.6
2-*cis*	261.0	261.0	289.3	284.0	106.7	154.2	154.2
18-*trans1*	266.3	264.9	286.0	283.4	105.1/105.0[c]	154.6	152.8
18-*trans2*	266.3	264.7	286.4	283.5	105.0/104.8	152.0	152.8
18-*cis1*	261.9	260.5	291.6	283.6	106.7/106.8	156.1	154.0
18-*cis2*	262.1	260.7	286.1	289.0	106.7/106.4	153.4	154.6
19-*trans*	265.7	265.7	288.5	283.1	105.1/104.9	152.2	154.6
19-*cis1*	261.3	261.3	293.7	283.3	106.8	155.8	155.8
19-*cis2*	261.7	261.7	288.3	288.6	106.5	153.9	153.9
21-*trans1*	265.7	265.7	285.5	285.5	105.1	154.6	154.6
21-*trans2*	265.5	265.5	286.1	286.1	104.9	152.1	152.1
21-*cis*	261.4	261.6	285.8	291.1	106.7/106.6	153.3	156.4
20-*trans*	267.0	264.1	285.7	286.0	105.0/105.1	154.0	152.9
20-*cis*	263.0	260.1	291.1	285.8	106.5/106.9	155.3	154.4
22-*trans1*	264.9	266.3	288.3	285.4	105.3/105.1	154.9	154.2
22-*trans2*	264.8	266.1	288.5	285.8	105.1/105.0	152.3	154.1
22-*cis1*	260.7	262.1	293.5	285.6	106.9/106.7	156.3	155.3
22-*cis2*	260.9	262.3	288.1	291.0	106.6/106.7	153.8	155.9
10-*trans*	265.8	265.8	287.9	287.9	105.1	154.2	154.2
10-*cis*	261.9	261.9	293.0	287.6	106.7	155.6	155.6

[a]Distances in picometers; [b]angles in degrees; [c]in *trans2* forms, NH1/NH2 correspond to N2H/N4H; in *cis2*, to N3H/N4H.

Table 3. Dipole moment values (in Debyes) calculated for different tautomeric forms of parent and *tert*-butyl-substituted porphycenes

2-trans	0.0
2-cis	1.15
18-trans1	0.80
18-trans2	0.62
18-cis1	1.78
18-cis2	0.85
19-trans	0.93
19-cis1	2.17
19-cis2	0.34
21-trans1	0.0
21-trans2	0.0
21-cis	1.27
20-trans	1.00
20-cis	1.59
22-trans1	0.55
22-trans2	0.73
22-cis1	1.78
22-cis2	1.02
10-trans	0.0
10-cis	1.36

reaction can proceed according to a stepwise mechanism. Such a possibility is also suggested by the form of the NH stretching vibrations. In porphycenes possessing the centre of inversion and equal values of N1N4 and N2N3 separation, the calculations yield an in-phase and an out-of-phase combinations of the NH stretches. The former should be observed by Raman, the latter, by IR spectroscopy. The mutual exclusion principle is no longer valid for **20**. The calculations for this molecule predict two separate bands of similar IR intensity, corresponding to the N1H and N3H stretches in the *trans* form (N1H and N2H in the *cis* species). In other words, the motions of the inner protons become decoupled after lowering of the overall molecular symmetry. It is crucial to note that the tautomerization potential in **20** still retains the symmetric double minimum character, the two *trans* and two *cis* forms being pairwise similar.

Loss of symmetry in porphycene derivatives should drastically influence the tunneling splitting due to the delocalization of two inner protons between the nitrogen atoms [29, 37, 53]. For this reason, *tert*-butyl-substituted porphycenes provide interesting objects for research on proton tunneling in supersonic jets. However, the consequences of symmetry changes may also be detected in condensed phase. Such effects may also be solvent-polarity-specific, since the calculations indicate different values of dipole moments in molecules for which the symmetry reduction destroys the pairwise degeneracy (Table 3).

Experimental demonstration of tautomerism in single molecules of *tert*-butyl-substituted porphycenes

In previous studies of **2** [36] and **10** [51], we have shown that tautomerism can be monitored on a single molecule level by observing the spatial pattern of the fluorescence from a single chromophore embedded in a thin polymer matrix. Due to the symmetry lowering expected for some *tert*-butyl derivatives, it seemed important to probe whether the reaction still proceeds in such molecules. Moreover, for chromophores located in a rigid polymer additional asymmetry due to the environemnt can also contribute to the decrease in the tautomerization rate. This may be the origin of the finding of Meixner and coworkers, who observed unusually long tautomerization times for single molecules of symmetric 2,3,7,8,12,13,17,18-octaethylporphyrin in polymer matrices [72].

Figure 4 presents the spatial patterns of the emission spectra of single molecules of **19** and **22** recorded in a thin (*ca*. 30 nm) poly(methyl methacrylate) film. To

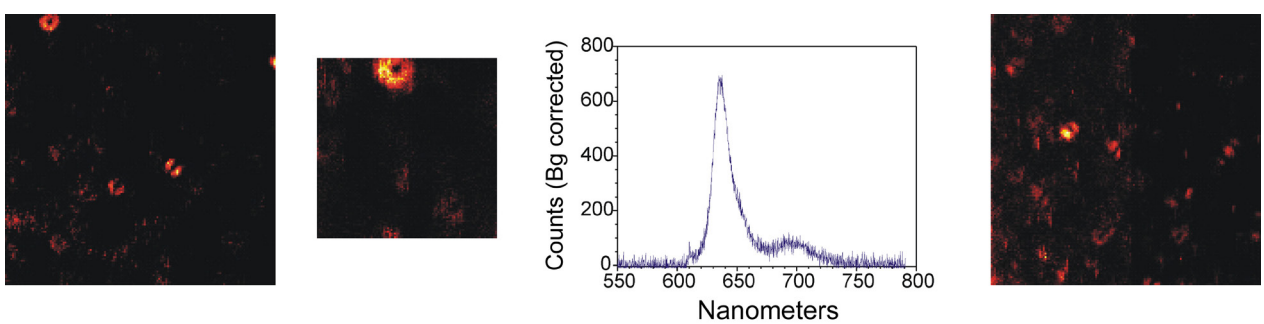

Fig. 4. (a) Image of room temperature fluorescence from single molecules of 2,7,12-tri-*tert*-butylporphycene **22** embedded in PMMA sheet, recorded from an area of 15 × 15 μm^2 with the azimuthal polarization of the exciting laser beam; (b) expanded view of the emission in the upper left corner of (a); (c) fluorescence spectrum from the molecule shown in (b); (d) fluorescence from single molecules of 2,7-di-*tert*-butylporphycene **19**

ensure that the emitting objects do really correspond to porphycenes, not only the total emission intensity was recorded, but also its spectral distribution, yielding fluorescence typical for porphycenes (Fig. 4c). The most important finding is the detection of ring shape patterns for both porphycenes. Such a shape is characteristic for a double–dipole emitter, *i.e.*, a molecule for which the S_1–S_0 transition cannot be represented by a single transition dipole. Double hydrogen transfer in porphycenes is usually accompanied by rotation of transition moments. A value of 72 ± 3° has been determined for the angle formed by the S_1–S_0 transition moment directions in the two *trans* tautomeric forms of the parent porphycene [36]. Similar results have been also observed for **10** [51]. The present findings demonstrate that tautomerization occurs at room temperature even for asymmetric porphycene derivatives. Moreover, the observation that the reaction in asymmetric **22** is accompanied by transition moment rotation is by no means trivial: in a recent study by Nonell and coworkers on another asymmetric derivative, 9-amino-2,7,12,17-tetraphenylporphycene, it was postulated that the transition dipoles do not change direction upon tautomerization [60].

For some molecules, not a ring, but a double-lobe emission pattern was observed. This can be explained by either (i) lack of tautomerization in certain molecules; (ii) different spatial orientation of the emitting chromophore, with its plane perpendicular to the plane of the sample. Our studies for **10** proved that the latter situation occurs. However, in the case of asymmetric porphycene the former explanation cannot be *a priori* excluded. Further studies are planned in this regard.

Syntheses of phenyl-substituted porphycenes

In 2008, Srinivasan and coworkers published the synthesis of porphycene using a novel, three-step procedure [73] based on acid-catalysed oxidative coupling of 2,2′-(1,2-diphenylethane-1,2-diyl)bis-1H-pyrrole. This method, however, seems to be limited only to a narrow group of *meso*-substituted porphycenes, which does not fully cover our expectations and, unfortunately, it failed in our hands. Therefore we decided to prepare this compound on a more classic route involving McMurry coupling of the proper diketone. One of the advantages of the *meso*-substituted porphycenes is that they can be obtained on a relatively short pathway, limited to, as in the method mentioned before, just three steps (Scheme 9). Thus, oxidative coupling of pyrrole mediated by phenyliodine(III) bis(trifluoroacetate) in the presence of bromotrimethylsilane afforded 2,2′-bipyrrole [74] which was immediately converted to the proper diphenyl ketone under Villsmeier–Haack conditions [75]. Further reaction under conditions elaborated by Vogel and coworkers [1] led to the expected 9,10,19,20-tetraphenyl porphycene (**25**) in 4% yield. Similarly, 9,20-diphenylporphycene (**26**) can be prepared by reaction of 5,5′-dibenzoyl-2,2′-bipyrrole (**27**) and 5,5′-diformyl-2,2′-bipyrrole (**23**), as it was confirmed by the MS analysis of the porphycene fraction isolated by column chromatography. However, separation of such formed product in a pure form from porphycene (**1**) and 9,10,19,20-tetraphenylporphycene (**26**), also obtained in this reaction, has not been so far completed, due to the very small difference in polarity of all of these compounds.

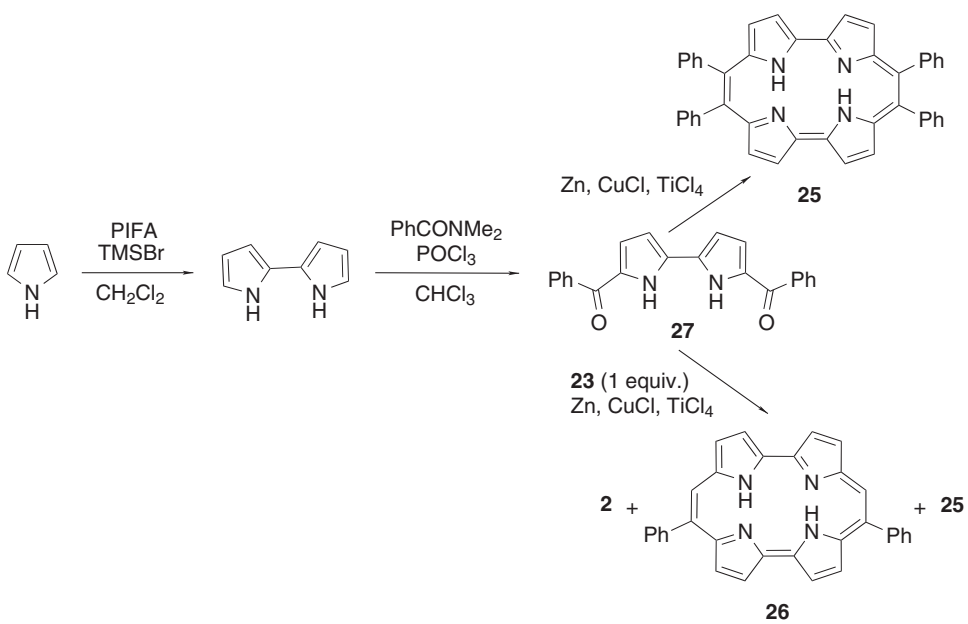

Scheme 9.

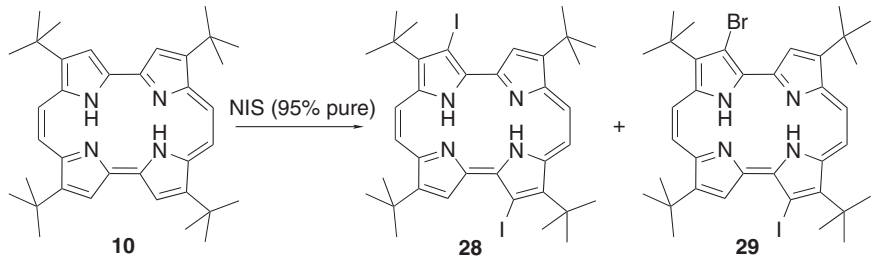

Scheme 10.

Synthesis and structure of halogenated porphycenes

The presence of a heavy atom in an organic molecule can increase the speed of all singlet–triplet conversion processes, both radiative and non-radiative. In order to enhance and explore the phenomenon of phosphorescence in porphycenes, we attempted to obtain halogen derivatives of porphycene. The first choice was 2,7,12,17-tetra-*tert*-butylporphycene (**10**), as the cheapest and most available substrate. The reaction was carried out using the *N*-iodosuccinimide (NIS) (95% pure) as a iodinating reagent. Because the iodination reaction is not selective, we received a very large number of products, but one of them deserves special attention. After a long and arduous process of separating a mixture of porphycene derivatives, it turned out that one of the purified reaction products had a mass corresponding to the product of substitution of two iodine atoms. NMR analysis demonstrated that the obtained compound is 3,13-diiodo-2,7,12,17-tetra-*tert*-butylporphycene (**28**) However, mass spectrometry analysis also revealed the existence of a compound with the mass corresponding to the product of substitution of one iodine atom and one ... bromine atom! It turned out that the reagent was not completely pure and contained the *N*-bromosuccinimide (NBS). It is known that the bromonium cation is more reactive than the iodonium cation, and thus, NBS reacted more rapidly than NIS. Not only mass spectra, but also careful NMR analysis confirmed that the obtained compound is 3-bromo-13-iodo-2,7,12,17-tetra-*tert*-butylporphycene (**29**) (Scheme 10). The crystallographic data could not be fully refined: in particular, it was difficult to distinguish bromine and iodine, most probably due to orientational disorder. In addition, the positions of the inner protons could not be determined. The latter effect, which can be due to both disorder and delocalization of the inner protons, has been known since the very first synthesis of parent porphycene [1]. Even though the X-ray data were not complete, they provided the unequivocal evidence for the 3,13-halogen positions on the porphycene ring.

An interesting effect has been observed during NMR studies of **29**. Based on the X-ray data, we expected to observe two singlet peaks due to inequivalent protons bonded to C6 and C16. Instead, two doublets were observed, each with the coupling constant of 2 Hz. The

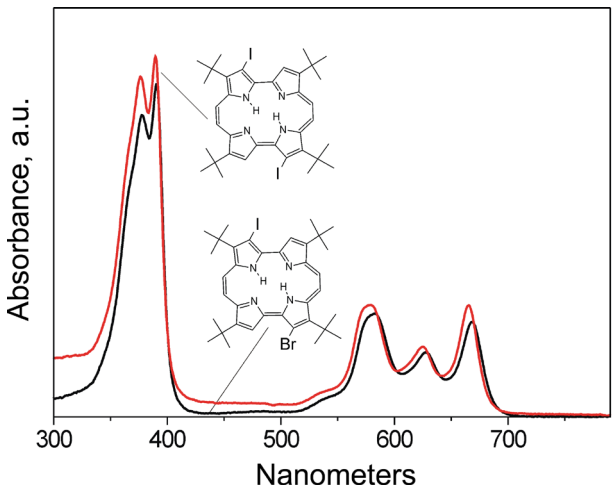

Fig. 5. The electronic absorption spectrum of 3,13-diiodo-2,7,12,17-tetra-*tert*-butylporphycene (**28**) (red) and 3-bromo-13-iodo-2,7,12,17-tetra-*tert*-butylporphycene (**29**) (black), recorded in acetone at 293 K

^{13}C spectrum exhibits 26 signals, suggesting a strong perturbation of symmetry by the presence of bromine and iodine in the molecule. Proton NMR spectra revealed a presence of two identical and two nonidentical *tert*-butyl groups. The latter are due to the presence of iodine or bromine atoms in the vicinity. This finding excluded the presence of two identical halogen atoms in the molecule, confirming the results from mass spectroscopy and X-ray studies.

More advanced 2D NMR investigations allowed to determine that the proton doublet splittings are due to the coupling of the C6 and C16 protons with the protons of the inner cavity. An analogous effect has been described by Vogel and coworkers for 2,3-dihydroporphycene [76].

In the electronic absorption spectra of halogenated derivatives (Fig. 5), a significant shift of the Q-bands towards the red (above 30 nm with respect to **10**) and a specific two-band shape in the Soret region were observed.

Structure and tautomerism of 3,13-dihalogenated-2,7,12,17-tetra-*tert*-butylporphycenes

B3LYP/6-311G(d,p) calculations performed for *trans* and *cis* tautomers of **28** and **29** reveal significant

Table 4. Calculated energy differences (in kcal/mol) between different tautomeric forms of **28** and **29**. See Table 1 for labeling conventions

	ΔE(*cis1-trans1*)	ΔE(*trans2-trans1*)	ΔE (*cis2-cis1*)
28	0.97 (0.58)	-3.97 (-3.95)	0
29	0.87 (0.72)	-3.89 (-3.46)	1.00 (0.86)

differences in energies and structure with regard to **10**, the non-halogenated derivative (Tables 4 and 5). First of all, the energies of two *trans* forms are no longer the same, the tautomeric species with protons located at N2 and N4 (*trans2*) being stabilized by nearly 4 kcal/mol with respect to the *trans*1 form. The geometry of the inner cavity also changes dramatically. The distances between hydrogen-bonded nitrogen atoms (N1N4 and N2N3) increase by more than 10 pm with respect to **10**, while the N1N2 and N3N4 separations become shorter by 5–7 pm. Thus, upon halogen substitution, the cavity becomes square-like, resembling that of porphyrin, but with a side length smaller by about 10 pm. We have recently demonstrated that tautomerization rate in porphyrin can be strongly accelerated by introducing substituents which make the inner cavity rectangular, similar in size to that of porphycenes [77]. The behavior caused by 3,13-dihalogen substitution is the opposite, showing a possibility of making porphyrin-like porphycenes by using appropriate substituents.

The computational results suggest a much weaker intramolecular hydrogen bonding for the halogenated derivatives **28** and **29** than in the corresponding non-halogenated compound. A consequence of this would be a much slower tautomerization rate. Actually, due to the considerable energy difference between the two *trans* forms, the inner protons may become localized in the *trans2* configuration. Finally, we note that in the more energetically stable *trans2* form all the inner geometry parameters (NHN and NH distances and NHN angles) suggest weaker hydrogen bonds than in *trans1* (Table 5). Thus, overall electronic effects caused by halogen substituents win over the energy gain obtained by forming stronger hydrogen bonds.

EXPERIMENTAL AND COMPUTATIONAL DETAILS

Electronic absorption spectra were recorded on a Shimadzu UV 3100 spectrophotometer. Single molecule measurements were performed using a home-built confocal scanning microscope equipped with a piezo nanopositioning stage (PI-517.3CD, Physik Instrumente). Higher order azimuthally polarized doughnut mode of a HeNe laser (λ = 594.1 nm) was generated by a polarization converter as described previously [78], and served as the excitation light source. The collimated beam was reflected by a dichroic beamsplitter (Z594RDC, Chroma) and focused by an oil immersion objective (CP-Achromat 100x/1.25 NA, Zeiss) onto the sample surface. Fluorescence from the sample was collected with the same objective, transmitted first through the dichroic beamsplitter mentioned above, and then through an emission filter (ET605LP, Chroma) for separation from scattered laser light and detected by a photon-counting avalanche photodiode (SPCM AQRH-14, Perkin Elmer). For spectral characterization the collected fluorescence was redirected to an EMCCD camera (Newton, Andor) equipped with an Andor Shamrock 303i spectrograph.

The calculations were carried out using Gaussian 09 program package (Revision B.01). Geometry optimizations have been performed using density functional theory, with the B3LYP functional and 6–31G(d,p) basis set. Vibrational structure has been calculated for each optimized stucture to ensure that no negative values of vibrational frequencies are present. For the bromine and iodine derivatives, the 6–311G(d,p) basis set was used [79].

2,2′-(*E*,*Z*)-ethene-1,2-diylbis(1*H*-pyrrole) (15)

Schlenk flask was charged under argon with the (*E*)-3-(1H-pyrrol-2-yl)-acrylic acid methyl ester (**14a**) (155 mg, 1 mmol) and 10 mL of freshly distilled benzene,

Table 5. Calculated geometries of the inner cavity for different tautomeric forms **28** and **29**. See Table 1 for labeling conventions

	N1N4	N2N3	N1N2	N3N4	NH1/NH2	N1HN4	N2HN3
28-*trans1*	276.5	276.5	281.7	281.7	104.1	152.2	152.2
28-*trans2*	278.2	278.2	281.6	281.6	103.2	149.4	149.4
28-*cis*	270.3	271.1	287.8	283.2	105.6/104.6	154.7	150.9
29-*trans1*	275.3	276.1	282.7	281.5	104.2/104.1	152.8	151.9
29-*trans2*	276.3	277.0	282.7	282.0	103.4/103.4	149.8	150.1
29-*cis1*	268.7	270.2	288.9	283.3	105.8/104.7	155.2	151.7
29-*cis2*	270.6	270.3	283.2	288.2	105.6/104.7	151.4	154.7

then indenylidene catalyst (48 mg, 0.05 mmol) was added. The reaction mixture was magnetically stirred at room temperature for 24 h under argon atmosphere. After completion of the reaction, the volatiles were removed under vacuum. The crude residue was purified by flash column chromatography (hexane/ethyl acetate 4:1) to give **15** (40 mg, 0.25 mmol, *E/Z* ratio 3/1). Spectral characteristics were in agreement with the data published previously [80].

Partial removal of *tert*-butyl groups from 2,7,12,17-tetra-*tert*-butylporphycene (10)

2,7,12,17-tetra-*tert*-butylporphycene (**10**, 100 mg, 0.187 mmol) was dissolved in concentrated H_2SO_4 (14 mL), then water (6 mL) was slowly added under argon. The mixture was heated at 150 °C for 10 min. 1-butanol (40 mL) and chloroform (200 mL) were added to the cold mixture, which was then neutralized with dilute NaOH and water. The solvent was removed under reduced pressure. The residue was extracted with CH_2Cl_2 The solution was evaporated. Porphycenes present in the mixture were separated by HPLC (hexane:THF:MeO′Bu 100:1:1).

2-*tert*-butylporphycene (18). ^{1}H NMR (200 MHz, $CDCl_3$): δ, ppm 10.17 (d, 1H, H-20, ^3J = 11.3 Hz), 9.83 (d, 1H, H-19, ^3J = 11.3 Hz), 9.80 (s, 2H, H-9, 10), 9.65 (m, 3H, H-6, 13, 16), 9.46 (d, 2H, H-3, ^4J = 1.4 Hz), 9.22 (m, 3H, H-7, 12, 17), 3.41 (br s, 1H, NH), 3.07 (br s, 1H, NH), 2.27 (s, 9H, ′Bu). UV-vis (acetonitrile): λ_{max}, nm 627.5, 594.5, 555.5, 372.5, 358.

2,7,12-tri-*tert*-butylporphycene (22). ^{1}H NMR (200 MHz, $CDCl_3$): δ, ppm 10.16 (s, 2H, H-9, 10), 10.11 (d, 1H, H-20, ^3J = 11.3 Hz), 9.77 (d, 1H, H-19, ^3J = 11.3 Hz)), 9.62 (d, 1H, H-16, ^3J = 4.1 Hz), 9.44; 9.42; 9.40 (3H, H-3, 6, 13), 9.18 (d, 1H, H-17, ^3J = 4.2 Hz), 3.58 (br s, 1H, NH), 3.28 (br s, 1H, NH), 2.27; 2.26; 2.25 (s, 3*9H, 3*′Bu). UV-vis (acetonitrile): λ_{max}, nm 629.5, 597, 558.5, 378.5, 364.

2,7-di-*tert*-butylporphycene (19)

To the suspension of Zn (2.615 g, 40 mmol) and CuCl (0.396 g, 4 mmol) in anhydrous THF (250 mL) $TiCl_4$*2THF (6.48 g, 20 mmol) was added slowly at 0 °C. The reaction mixture was heated to the reflux for 3 h and 1H,1′H-[2,2′]bipyrrolyl-5,5′-dicarbaldehyde (**23**, 0.186 g, 1 mmol) and 4,4′-di-*tert*-butyl-1H,1′H-[2,2′] bipyrrolyl-5,5′-dicarbaldehyde (**24**, 0.300 g, 1 mmol) were added quickly. Heating was prolonged for additional 2 h, then the reaction mixture was cooled down to room temperature and ammonia solution (*ca*. 10%, 200 mL) was added. Such resulted mixture was stirred in air overnight, then it was filtered through Celite pad, which was additionally washed with THF (3 × 70 mL). Organic solvents were removed from the filtrate under reduced pressure and the residue was extracted with CH_2Cl_2 (3 × 70 mL). The organic layer was dried over anhydrous Na_2SO_4, crude product was isolated by column chromatography (hexane:ethyl acetate 4:1) to give **19** (8 mg, 0.02 mmol) as a blue solid. ^{1}H NMR (200 MHz, $CDCl_3$): δ, ppm 10.15 (d, 2H, H-9, 20, ^3J = 11.3 Hz), 9.80 (d, 2H, H-10, 19, ^3J = 11.3 Hz), 9.52 (d, 2H, H-13, 16, ^3J = 4.4 Hz), 9.44 (d, 2H, H-3, 6, ^4J = 0.9 Hz), 9.21 (d, 2H, H-12, 17, ^3J = 4.4 Hz), 3.38 (br s, 2H, NH), 2.25 (s, 18H, 2*′Bu). UV-vis (acetonitrile): λ_{max}, nm 627.5, 596.5, 558, 375, 362.

9,10,19,20-tetraphenylporphycene (25)

To the suspension of Zn (7.26 g, 111 mmol) and CuCl (1.13 g, 11.1 mmol) in anhydrous THF (250 mL) $TiCl_4$ (6.30 mL, 55.4 mmol) was added slowly at 0 °C. The reaction mixture was heated to the reflux for 1 h and 5,5′-dibenzoyl-2,2′-bipyrrole (**27**, 0.942 g, 2.77 mmol) was added quickly. Heating was prolonged for additional 2 h, then reaction mixture was cooled down to room temperature and ammonia solution (*ca*. 10%, 200 mL) was added. Such resulted mixture was stirred on air overnight, then it was filtered through Celite pad, which was additionally washed with THF (3 × 70 mL). Organic solvents were removed from the filtrate under reduced pressure and the residue was extracted with CH_2Cl_2 (3 × 70 mL). The organic layer was dried over anhydrous Na_2SO_4, filtered through silica pad (hexane: CH_2Cl_2; 7:3) and finally the expected product was isolated by column chromatography (hexane:CH_2Cl_2 7:3) to give **25** (34 mg, 0.053 mmol) as a blue solid. The spectral characteristics were in agreement with the data published previously [73].

Iodination of 2,7,12,17-tetra-*tert*-butylporphycene (10)

2,7,12,17-tetra-*tert*-butylporphycene (**10**, 30 mg, 0.056 mmol) was dissolved in 5 mL of THF, then NIS (18.96 mg, 0.084 mmol) was added slowly to the intensively stirred solution. After addition stirring was continued for 1 h. The reaction mixture was evaporated and chromatographed on silica gel (eluent hexane/ CH_2Cl_2 3:1), followed by another chromatography (eluent hexane) to give **28** (5.1 mg 0.0069 mmol) and **29** (6.7 mg 0.0085 mmol).

3,13-diiodo-2,7,12,17-tetra-*tert*-butylporphycene (28). ^{1}H NMR (500 MHz, $CDCl_3$): δ, ppm 10.85 (d, 2H, H-6,16, ^4J = 2.2 Hz), 10.33 (d, 2H, H-10,20, ^3J = 12.0 Hz), 9.96 (d, 2H, H-9,10, ^3J = 12.0 Hz), 2.42 (s, 18H, 2x′Bu, C-2, 12), 2.23 (s, 18H, 2x′Bu, C-7, 17). ^{13}C NMR (500 MHz, $CDCl_3$): δ, ppm 155.29, 150.55, 149.53, 138.93, 135.30, 129.65, 123.21, 115.38, 109.77, 82.31, 36.62, 35.51, 34.44, 33.74. MS (ESI): *m/z* 787 [M + H$^+$]. UV-vis (acetone): λ_{max}, nm 378, 391, 580, 626, 668.

3-bromo-13-iodo-2,7,12,17-tetra-*tert*-butylporphycene (29). ^{1}H NMR (500 MHz, $CDCl_3$): δ, ppm 10.86 (d, 1H, H-6, ^4J = 2.2 Hz), 10.49 (d, 1H, H-16, ^4J = 2.2 Hz), 10.36 (d, 1H, H-20, ^3J = 12.0 Hz), 10.28 (d, 1H,

H-10, ^3J = 11.9 Hz), 10.00 (d, 1H, H-9, ^3J = 12.4 Hz), 9.97 (d, 1H, H-19, ^3J = 12.8 Hz), 2.43 (s, 9H, ^{t}Bu, C-2), 2.37 (s, 9H, C-12), 2.24 (s, 18H, C-7,17), 1.39 (br s, 1H, NH), 1.32 (br s, 1H, NH). ^{13}C NMR (500 MHz, $CDCl_3$): δ, ppm 155.20, 150.96, 150.60, 150.29, 149.36, 148.65, 138.78, 136.49, 135.39, 135.25, 129.68, 128.86, 123.23, 122.38, 115.63, 115.42, 114.08, 110.10, 109.83, 82.34, 36.64, 36.53, 35.51, 34.66, 34.35, 33.62. MS (ESI): *m/z* 741.2 [M + H$^+$]. UV-vis (acetone): λ_{max}, nm 376, 390, 578, 624, 665.

SUMMARY AND PERSPECTIVES

The new porphycenes will be used as objects in studies encompassing at least five different research areas. The first two are spectroscopy and photophysics. Regarding the former, it should be recalled that, due to the "hard-chromophore" nature of porphycene chromophore (ΔHOMO << ΔLUMO), substitution should not strongly affect the intensity of the electronic transitions [9, 24]. On the other hand, the transition energy can be shifted by suitable substitution. For instance, in *meso*-alkyl- or aryl-substituted porphycenes, the origin of the electronic absorption is red-shifted with respect to the unsubstitued chromophore by more than 30 nm. Interestingly, the second transition seems to be shifted more than the first one, which leads to the coalescence of two transitions, resulting in the broadening of the lowest absorption band. Initial studies for the doubly *meso*-substituted derivatives show that the red shift is roughly about half that observed for tetrasubstituted porphycenes. In contrast to the latter, the S_1–S_2 separation seems to be preserved.

Regarding photophysics, comparison of the excited state depopulation patterns in *meso* doubly- and tetrasubstituted derivatives will be a crucial test for a recently suggested mechanism of excited state depopulation in porphycenes [52]. According to this model, the deactivation channel involves both twisting of two pyrrole units and a single hydrogen transfer from a *trans* to a *cis* tautomer, the latter with two protons on separate bipyrrole moieties. A consequence of this mechanism is a large viscosity dependence of fluorescence quantum yields and lifetimes in *meso*-tetraalkylsubstituted derivatives [56]. The model predicts a much weaker dependence for the 9,10,19,20-tetraphenylporphycene **25** and for doubly-substituted derivatives. Preliminary measurements reveal much stronger fluorescence in all these compounds.

Porphycenes are particularly suitable for studies of intramolecular hydrogen bonding and tautomerism, because the strength of their hydrogen bonds may be strongly altered by substituents, due to changes in size of the internal cavity. Extremely instructive are the measurements performed for ultracold molecules isolated in supersonic jets [29, 37] or helium nanodroplets [53]. Such studies allow to pinpoint mode-dependent tunneling splittings due to coherent delocalization of two internal protons. Very promising in this regard are the singly, doubly, and triply *tert*-butyl-substituted derivatives **18**–**22**, of which the structure has been discussed above. Investigations of these molecules by high-resolution spectroscopy techniques should contribute to the understanding of such phenomena as the role of symmetry in tunneling splitting, coupling of low and high frequency modes involved in hydrogen bond, cooperativity in double hydrogen transfer, and the influence of conformational isomerism on the tunneling characteristics. Compounds **18–22** bridge a gap between the parent porphycene and 2,7,12,17-tetra-*tert*-butylporphycene **10**. Supersonic jet studies of the latter [35] revealed a very complicated pattern of vibronic transitions, making it very difficult to distinguish features due to tunneling from the contributions of different conformers. Such distinction may become possible by carrying out systematic studies of singly, doubly and triply-substitued compounds.

All the newly obtained porphycenes will be screened against their photooxidizing properties. It has been demonstrated many times that minor structural variations can lead to huge changes in phototherapeutic activity [20]. A systematic study of such variations will be possible for the series of **10**, **18**–**22**. These group of compounds will also enable a particularly challenging, but possibly rewarding task: getting insight into differences in spectral and photophysical behavior along the series on a single molecule level. For this, we plan to combine fluorescence, Raman, and atomic and tunneling microscopy techniques.

In summary, it can be stated without any doubt that the pioneering work on porphycene isomers initiated by Emanuel Vogel and his coworkers a quarter of century ago has been providing inspiration, fascination, and fun for many researchers from diverse areas. The field is growing, and one can expect exciting news in the years to come.

Acknowledgements

The authors thank Dr. Roman Luboradzki for the X-ray structures of halogenated porphycenes. The research was partially supported by the European Union within European Regional Development Fund, through grant Innovative Economy (POIG.01.01.02-00-008/08), and by the Ministry of Science and Higher Education grants, PBZ/MNiSW07/2006/44-PolPostdoc III Project and N N204 355040. We acknowledge the computing grant (No. G17–14) from the Interdisciplinary Centre for Mathematical and Computational Modeling of the Warsaw University. We are grateful to Prof. A. Meixner for providing us with blueprints of a confocal microscope.

REFERENCES

1. Vogel E, Köcher M, Schmickler H and Lex J. *Angew. Chem., Int. Ed. Engl.* 1986; **25**: 257–259.
2. Vogel E. *Pure Appl. Chem.* 1990; **62**: 557–564.

3. Vogel E. *Pure Appl. Chem.* 1996; **68**: 1355–1360.
4. Vogel E. *J. Heterocycl. Chem.* 1996; **33**: 1461–1487.
5. Sessler JL. *Angew. Chem.* 1994; **33**: 1348–1350.
6. Wu YD, Chan KWK, Yip CP, Vogel E, Plattner DA and Houk KN. *J. Org. Chem.* 1997; **62**: 9240–9250.
7. Sessler JL, Gebauer A and Vogel E. In *The Porphyrin Handbook*, Vol. 2, Kadish KM, Smith KM and Guilard R. (Eds.) Academic Press: 2000; pp 1–59.
8. Sánchez-Garcia D and Sessler JL. *Chem. Soc. Rev.* 2008; **37**: 215–232.
9. Waluk J. In *Handbook of Porphyrin Science*, Vol. 7, Smith K, Kadish K and Guilard R. (Eds.) World Scientific: 2010; pp 359–435.
10. Waluk J and Michl J. *J. Org. Chem.* 1991; **56**: 2729–2735.
11. Callot HJ, Metz B and Tschamber T. *New J. Chem.* 1995; **19**: 155–159.
12. Vogel E, Bröring M, Weghorn SJ, Scholz P, Deponte R, Lex J, Schmickler H, Schaffner K, Braslavsky SE, Müller M, Pörting S, Fowler CJ and Sessler JL. *Angew. Chem., Int. Ed. Engl.* 1997; **36**: 1651–1654.
13. Aukauloo MA and Guilard R. *New J. Chem.* 1994; **18**: 1205–1207.
14. Sessler JL, Brucker EA, Weghorn SJ, Kisters M, Schafer M, Lex J and Vogel E. *Angew. Chem., Int. Ed. Engl.* 1994; **33**: 2308–2312.
15. Vogel E, Bröring M, Erben C, Demuth R, Lex J, Nendel M and Houk KN. *Angew. Chem., Int. Ed. Engl.* 1997; **36**: 353–357.
16. Vogel E, Scholz P, Demuth R, Erben C, Broring M, Schmickler H, Lex J, Hohlneicher G, Bremm D and Wu YD. *Angew. Chem.-Int. Edit.* 1999; **38**: 2919–2923.
17. Chmielewski PJ, Latos-Grażyński L, Rachlewicz K and Glowiak T. *Angew. Chem., Int. Ed. Engl.* 1994; **33**: 779–781.
18. Furuta H, Asano T and Ogawa T. *J. Am. Chem. Soc.* 1994; **116**: 767–768.
19. Battersby AR, Fookes CJR, Matcham GWJ and McDonald E. *Nature (London)* 1980; **285**: 17–21.
20. Stockert JC, Cañete M, Juarranz A, Villanueva A, Horobin RW, Borrell J, Teixidó J and Nonell S. *Curr. Med. Chem.* 2007; **14**: 997–1026.
21. Richert C, Wessels JM, Müller M, Kisters M, Benninghaus T and Goetz AE. *J. Med. Chem.* 1994; **37**: 2797–2807.
22. Braslavsky SE, Müller M, Mártire DO, Pörting S, Bertolotti SG, Chakravorti S, Koç-Weier G, Knipp B and Schaffner K. *J. Photochem. Photobiol. B* 1997; **40**: 191–198.
23. Wehrle B, Limbach HH, Kocher M, Ermer O and Vogel E. *Angew. Chem., Int. Ed. Engl.* 1987; **26**: 934–936.
24. Waluk J, Müller M, Swiderek P, Köcher M, Vogel E, Hohlneicher G and Michl J. *J. Am. Chem. Soc.* 1991; **113**: 5511–5527.
25. Waluk J and Vogel E. *J. Phys. Chem.* 1994; **98**: 4530–4535.
26. Malsch K and Hohlneicher G. *J. Phys. Chem. A* 1997; **101**: 8409–8416.
27. Malsch K, Roeb M, Karuth V and Hohlneicher G. *Chem. Phys.* 1998; **227**: 331–348.
28. Kozlowski PM, Zgierski MZ and Baker J. *J. Chem. Phys.* 1998; **109**: 5905–5913.
29. Sepioł J, Stepanenko Y, Vdovin A, Mordziński A, Vogel E and Waluk J. *Chem. Phys. Lett.* 1998; **296**: 549.
30. Frydman B, Fernandez CO and Vogel E. *J. Org. Chem.* 1998; **63**: 9385–9391.
31. Langer U, Hoelger C, Wehrle B, Latanowicz L, Vogel E and Limbach HH. *J. Phys. Org. Chem.* 2000; **13**: 23–34.
32. Gil M, Jasny J, Vogel E and Waluk J. *Chem. Phys. Lett.* 2000; **323**: 534.
33. Ghosh A, Moulder J, Bröring M and Vogel E. *Angew. Chem., Int. Ed. Engl.* 2001; **40**: 431–434.
34. Kay CWM, Gromadecki U, Törring JT and Weber S. *Mol. Phys.* 2001; **99**: 1413–1420.
35. Nosenko Y, Jasny J, Pietraszkiewicz M and Mordziński A. *Chem. Phys. Lett.* 2004; **399**: 331–336.
36. Piwoński H, Stupperich C, Hartschuh A, Sepioł J, Meixner A and Waluk J. *J. Am. Chem. Soc.* 2005; **127**: 5302–5303.
37. Vdovin A, Sepioł J, Urbańska N, Pietraszkiewicz M, Mordziński A and Waluk J. *J. Am. Chem. Soc.* 2006; **128**: 2577–2586.
38. Waluk J. *Acc. Chem. Res.* 2006; **39**: 945–952.
39. Walewski L, Krachtus D, Fischer S, Smith JC, Bala P and Lesyng B. *Int. J. Quantum Chem.* 2006; **106**: 636–640.
40. Walewski Ł, Bała P and Lesyng B. In *From Computational Biophysics to Systems Biology (CBSB07),* Proceedings of the NIC Workshop 2007, Vol. 36, Hansmann UHE, Meinke J, Mohanty S and Zimmermann O. (Eds.) John von Neumann Institute for Computing: Jülich, NIC Series, 2007; pp 291–295 (ISBN 978–3-9810843–2-0, http://www.fz-juelich.de/nic-series/volume36).
41. Gil M, Organero JA, Waluk J and Douhal A. *Chem. Phys. Lett.* 2006; **422**: 142–146.
42. Gil M and Waluk J. *J. Am. Chem. Soc.* 2007; **129**: 1335–1341.
43. Pietrzak M, Shibl MF, Broring M, Kühn O and Limbach HH. *J. Am. Chem. Soc.* 2007; **129**: 296–304.
44. Waluk J. In *Hydrogen-Transfer Reactions*, Vol. 1, Hynes JT, Klinman JP, Limbach HH and Schowen RL. (Eds.) Wiley-VCH: Weinheim, 2007; pp 245–271.
45. Shibl MF, Pietrzak M, Limbach HH and Kühn O. *ChemPhysChem* 2007; **8**: 315–321.

46. Smedarchina Z, Shibl MF, Kühn O and Fernández-Ramoz A. *Chem. Phys. Lett.* 2007; **426**: 314–321.
47. Smedarchina Z, Siebrand W, Fernandez-Ramos A and Meana-Paneda R. *Z. Phys. Chemie-Int. J. Res. Phys. Chem. Chem. Phys.* 2008; **222**: 1291–1309.
48. Fita P, Urbańska N, Radzewicz C and Waluk J. *Z. Phys. Chem. (Munich)* 2008; **222**: 1165–1173.
49. Fita P, Urbańska N, Radzewicz C and Waluk J. *Chem. — Eur. J.* 2009; **15**: 4851–4856.
50. Lopez del Amo J, Langer U, Torres V, Pietrzak M, Buntkowsky G, Vieth HM, Shibl MF, Kühn O, Bröring M and Limbach HH. *J. Phys. Chem. A* 2009; **113**: 2193–2206.
51. Piwoński H, Hartschuh A, Urbańska N, Pietraszkiewicz M, Sepioł J, Meixner A and Waluk J. *J. Phys. Chem. C* 2009; **113**: 11514–11519.
52. Sobolewski A, Gil M, Dobkowski J and Waluk J. *J. Phys. Chem. A* 2009; **113**: 7714–7716.
53. Vdovin A, Waluk J, Dick B and Slenczka A. *ChemPhysChem* 2009; **10**: 761–765.
54. Walewski Ł, Waluk J and Lesyng B. *J. Phys. Chem. A* 2010; in press.
55. Waluk J. *Isr. J. Chem.* 2009; **49**: 175–185.
56. Gil M, Dobkowski J, Wiosna-Sałyga G, Urbańska N, Fita P, Radzewicz C, Pietraszkiewicz M, Borowicz P, Marks D, Glasbeek M and Waluk J. *J. Am. Chem. Soc.* 2010; **132**: 13472–13485.
57. Yoshikawa T, Sugawara S, Takayanagi T, Shiga M and Tachikawa M. *Chem. Phys. Lett.* 2010; **496**: 14–19.
58. Abdel-Latif MK and Kühn O. *Theor. Chem. Acc.* 2011; **128**: 307–316.
59. Fita P, Garbacz P, Nejbauer M, Radzewicz C and Waluk J. *Chem. — Eur. J.* 2011; **17**: 3672–3678.
60. Duran-Frigola M, Tejedor-Estrada R, Sánchez-García D and Nonell S. *Phys. Chem. Chem. Phys.* 2011; **13**: 10326–10332.
61. Schlabach M, Wehrle B, Rumpel H, Braun J, Scherer G and Limbach HH. *Ber. Bunsen-Ges. Phys. Chem.* 1992; **96**: 821–833.
62. Braun J, Schlabach M, Wehrle B, Köcher M, Vogel E and Limbach HH. *J. Am. Chem. Soc.* 1994; **116**: 6593–6604.
63. Braun J, Limbach HH, Williams PG, Morimoto H and Wemmer DE. *J. Am. Chem. Soc.* 1996; **118**: 7231–7232.
64. Vogel E, Balci M, Pramod K, Koch P, Lex J and Ermer O. *Angew. Chem., Int. Ed. Engl.* 1987; **26**: 928–931.
65. Lausmann M, Zimmer I, Lex J, Lueken H, Wieghardt K and Vogel E. *Angew. Chem., Int. Ed. Engl.* 1994; **33**: 736–739.
66. Urbańska N, Pietraszkiewicz M and Waluk J. *J. Porphyrins Phthalocyanines* 2007; **11**: 596–600.
67. Neya S and Funasaki N. *Tetrahedron Lett.* 2002; **43**: 1057–1058.
68. Neya S, Quan J, Hoshino T, Hata M and Funasaki N. *Tetrahedron Lett.* 2004; **45**: 8629–8630.
69. Morimoto T, Taniguchi S, Osuka A and Furuta H. *Eur. J. Org. Chem.* 2005; **18**: 3887–3890.
70. Berlin A, Bradamante S, Ferraccioli R, Pagani GA and Sannicolò F. *J. Chem. Soc., Perkin Trans.* 1987; **1**: 2631–2635.
71. Garcia-Rubia A, Arrayás RG and Carretero JC. *Angew. Chem. Int. Ed.* 2009; **48**: 6511–6515.
72. Chizhik AM, Jäger R, Chizhik AI, Bär S, Mack HG, Sackrow M, Stanciu C, Lyubimtsev A, Hanack M and Meixner AJ. *Phys. Chem. Chem. Phys.* 2011; **13**: 1722–1733.
73. Anju KS, Ramakrishnan S, Thomas AP, Suresh E and Srinivasan A. *Org. Lett.* 2008; **10**: 5545–5548.
74. Dohi T, Morimoto K, Ito M and Kita Y. *Synthesis* 2007: 2913–2917.
75. Braaten KC, Gordon DG, Aphibal MM and Geier GR. *Tetrahedron* 2008; **64**: 9828–9836.
76. Vogel E, Köcher M, Balci M, Teichler I, Lex J, Schmickler H and Ermer O. *Angew. Chem., Int. Ed. Engl.* 1987; **26**: 931–934.
77. Gawinkowski S, Orzanowska G, Izdebska K, Senge MO and Waluk J. *Chem. — Eur. J.* 2011; **17**: 10039–10049.
78. Dorn R, Quabis S and Leuchs G. *Phys. Rev. Lett.* 2003; **91**: 233901–233904.
79. a) Krishnan R, Binkley JS, Seeger R and Pople JA. *J. Chem. Phys.* 1980; **72**: 650–654. b) Curtiss LA, McGrath MP, Blandeau JP, Davis NE, Binning RC Jr. and Radom L. *J. Chem. Phys.* 1995; **103**: 6104–6113. c) Glukhovstev MN, Pross A, McGrath MP and Radom L. *J. Chem. Phys.* 1995; **103**: 1878–1885; Erratum: *J. Chem. Phys.* 1996; **104**: 3407.
80. Pagani G, Berlin A, Canavesi A, Schiavon G, Zecchin S and Zotti G. *Adv. Mater.* 1996; **8**: 819–823.